The Weldability Evaluation of Dissimilar Welds of AISI 347 Stainless Steel to ASTM A335 Low Alloy Steel by Gas Tungesten Arc Welding

I. Hajiannia[a,*], M. Shamanian[b], M. Kasiri[a]

[a] *Department of Materials Engineering, Najafabad Branch, Islamic Azad University, Isfahan, Iran.*
[b] *Department of Materials Engineering, Isfahan University of Technology, Isfahan, Iran.*

ARTICLE INFO

Article history:

Received 27 Aug 2013
Accepted 01 Dec 2013
Available online 25 Dec. 2013

Keywords:

Dissimilar welding
Austenitic stainless steel
Low alloy steels
Weldability
Microstructure

ABSTRACT

In the present study, the weldability and microstructure of dissimilar welds of AISI 347 austenitic stainless steel to ASTM A335 low alloy steel was investigated. For this purpose, gas tungsten arc welding process and two filler metals including ERNICr-3 and ER309L were used. After welding, the microstructure of the different zones of each joint, including weld metals, heat affected zone (HAZ)(Heat Affected Zone), interface and unmixed zones (UMZ)(Unmixed Zone) was evaluated by using optical microscopy. The scanning electron microscopy (SEM)(Scanning Electron Microscopy) equipped with energy disperse spectrometry (EDS)(Energy Dispersive Spectroscopy) was used to investigate the precipitates, in order to predict the micro structure of weld metal and transmission zone in dissimilar joints. In ERNiCr-3 weld metal, the solidification was observed as the completely austenitic and equiaxed dendrite(Dendrite) which contains the precipitates of carbide complex, as well as Niobium segregation happened in the inter dendrite zones. 309L weld metal was observed as the primary ferrite with austenitic matrix and microstructure was seen as skeletal ferrite morphology. The epitaxial growth was observed in the interface between 347 austenitic stainless steel and two filler metals and a narrow zone was observed in the interface between A335 low alloy steel and filler metals; moreover, coarse grains appeared in HAZ zone of both weld metals. Finally, it can be denoted that for the joints between the AISI 347 austenitic stainless steel and A335 low alloy steel, the ERNICr-3 filler material provides the optimum qualities.

1. Introduction

Stainless steels are ferrous alloys containing at least 10 to 12 percent chromium. 347 austenitic stainless steel is one of the most common types of steel used in industries, especially in oil and gas industry, refinery and electric power stations because of its corrosion resistance to water environments and high temperatures [1]. This alloy has good resistance to intergranular(Intergranular Corrosion) corrosion in many corrosive environments [2, 3]. Chromium-molybdenum low alloy steels are other types of steel which are resistant to

Corresponding author:
E-mail address: Iman_hajiannia@yahoo.com (Iman Hajiannia).

Table 1. Nominal chemical composition of materials used (Wt%)

Fe	Nb	Ag	Cu	Ti	Si	Mn	Mo	Ni	Cr	C	Element
BAL	-	0.16	0.08	-	1.0	0.3	0.5	-	1.12	0.1	A335
BAL	0.55	0.12	0.35	0.01	1.0	2.0	0.37	10.65	17.36	0.08	AISI 347
BAL	-	-	0.05	-	0.51	1.8	0.04	13.9	23.7	0.02	ER309L
3	3	3	0.12	.05	0.75	0.5	3	BAL	16	0.1	ERNiCr-3

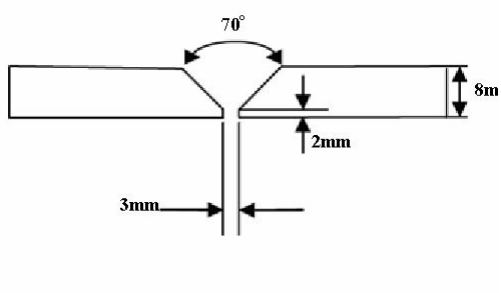

Fig. 1. The pipe connection.

erosion and corrosion. These steels are mostly used in producing gearwheels, steam utilities, petroleum and power stations [1]. Dissimilar joint of 347 austenitic stainless steel and A335 low alloy steel pipes has been widely employed in the oil and gas industry especially in heat exchangers. In dissimilar welding, one of the most important concerns is the selection of a proper filler material. In recent years, some studies on the evaluation of dissimilar welding of stainless steel and low alloy steel have been conducted.

Arivazhagan(Arivazhagan), et al. [4] studied the effect of heat input on the microstructure and mechanical properties of welding sections of 304 austenitic stainless steel and 4140 low alloy steel by gas tungsten arc welding (GTAW). The results showed that high heat input enhanced the micro-segregation of alloy elements and created a non-chromium zone in the grain boundaries; therefore, the mechanical properties of the joints deteriorated.

Klueh(Klueh)[5] investigated the failure of a transferred joint between 2.25 Cr-1Mo steel and 321austenitic stainless steel which was made by using Ni-based Inconel 182 filler metal. It was illustrated that after heating this joint in high temperatures for 10 to 15 years, the heat-affected zone contained large ferrite grains; consequently, cracking happened in this zone. However, no systematic work has been conducted on the joint between 347 austenitic stainless steel and A335 low alloy steel pipes. The aim of this study is to investigate the mechanical properties and microstructure of different welding zones in order to find the best filler metal with the proper engineering properties for these dissimilar joints.

2. Experimental

The base metals used in this study were A335 low alloy steel and 347 austenitic stainless steel pipes which were under rolled and solution annealed conditions, respectively [6]. The pipes were 8 mm thick and 200 mm in outer diameter. Two filler metals, ER309L and ERNiCr-3, were used to join the base metals [7]. The nominal chemical compositions of the base and filler metals are given in table 1. Wires 2.4 mm in diameter were used for root pass and hot and cover passes. Before welding, the pipes were prepared to make a single V groove butt configuration. Fig 1 shows the pipe connection. The welding was done by gas tungsten arc welding process with Direct-Current Electrode Negative (GTAW-DCEN) and argon gas shield of 99.99% purity. The inter-pass temperature was selected 150°C in order to minimize the tension of the weld metal solidification. The heat input was calculated by the following equation:

$$H.I = \eta.I.V/S \qquad \eta = 0.6 \qquad [1]$$

The welding parameters and the heat input in each welding pass are given in table 2. Two specimens with proper size were prepared by grinding using 80 to 2000 grits silicon carbide paper, followed by final polishing with 0.3 μm alumina powders. The specimens were etched for 15 seconds using Nital solution (2% nitrate acid in alcohol) to show the structure of low alloy steel; also, they were etched by Marbel solution (10 gr of $CuSO_4$ + 50cc HCI + 50cc H_2O) to find the microstructure of austenitic stainless steel weld metal. The specimens were elecroetched by a solution (60 ml water and 40

Table 2. Specifications of gas tungsten arc welding.

Welding Parameters					
Heat Input ($kJmm^{-1}$)	Welding Speed (mms^{-1})	Volt (V)	Amper (A)	Pass No.	Filler Metal
0.981	1.1	12	150	1	
0.840	1.0	10	140	2	
0.709	1.1	11	130	3	ER309L
0.720	1.1	12	110	4	
0.818	1.1	10	150	1	
0.840	1.0	10	140	2	ERNiCr-3
0.840	1.0	10	140	3	
0.715	1.2	11	130	4	

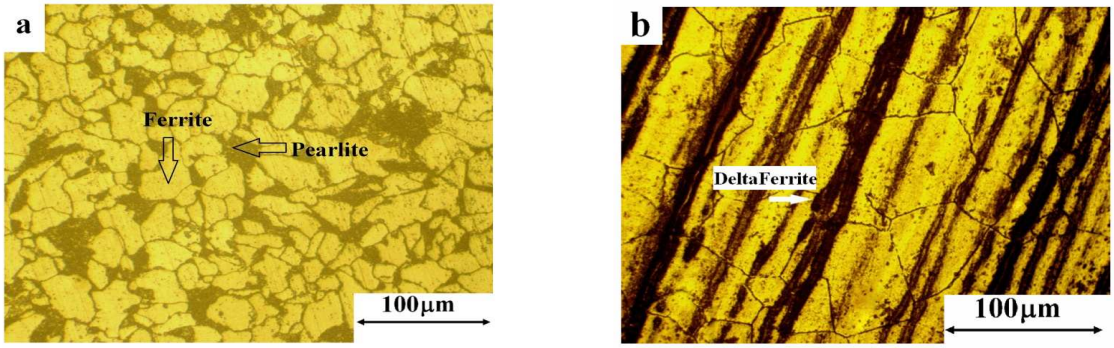

Fig. 2. Microstructure of base materials (a) low-alloy steel A335, (b) austenitic stainless steel 347.

ml nitrate acid), with 5 volts for 10 seconds; as a result, the microstructure of nickel-based weld metal was found. The microstructure of different weld areas was examined by (CK40M Olympus) optical microscope at different magnifications. A scanning electron microscope (Zeiss) equipped with chemical analysis was used to study the microstructure.

3. Results and Discussion

Fig 2(a) shows the microstructure of A335 chromium-molybdenum low alloy steel in which ferrite grains (10 μm) with dark pearlite grains (14 μm) can be observed [9]. The microstructure of 347 austenitic stainless steel contains an austenitic field with equiaxed grains (75 μm) as shown in Fig 2(b). The microstructure of 309L austenitic stainless steel weld metal (which was related to the root pass) is shown in Fig 3(a) and (b). The solidification of 309L as a primary ferrite (δ)(Delta Ferrite) exhibited a skeletal ferrite morphology and solidification of FA type [3]. The ferrite content of the root pass of 309L filler metal was about 5.7% (by a ferritescope). The granular structure of ERNiCr-3 weld metal which is related to the root pass is shown in Fig 4. The weld metal ERNiCr-3 contains about 67 wt. % nickel and its solidification is fully austenitic. Also, a two-phase structure, which contains dendrite and interdendrite zones, can be observed. This weld metal contains 3% Nb which can stabilize austenite at high temperatures and also increase the solidification temperature range [1]. The scanning electron microscopy was used for more precise examination of weld microstructure. Small white precipitates which were sometimes segregated clearly from the field were observed in the interdendritic region. Fig 5 (a) shows the SEM micrographs of ERNiCr-3 weld metal, Fig 5 (b) displays the precipitates of ERNiCr-3 weld metal, and Fig 6 shows the EDS results analysis of the precipitates. These precipitates do not have certain geometric forms, and their lengths are about 2 microns. They are enriched with Nb and are formed as NbC carbides. Also, there is some Ti in the EDS results analysis [1, 11]. The equivalent chromium and nickel were calculated by Schaeffler(Schaeffler) equations. Table 3 shows the calculated amounts for equivalent

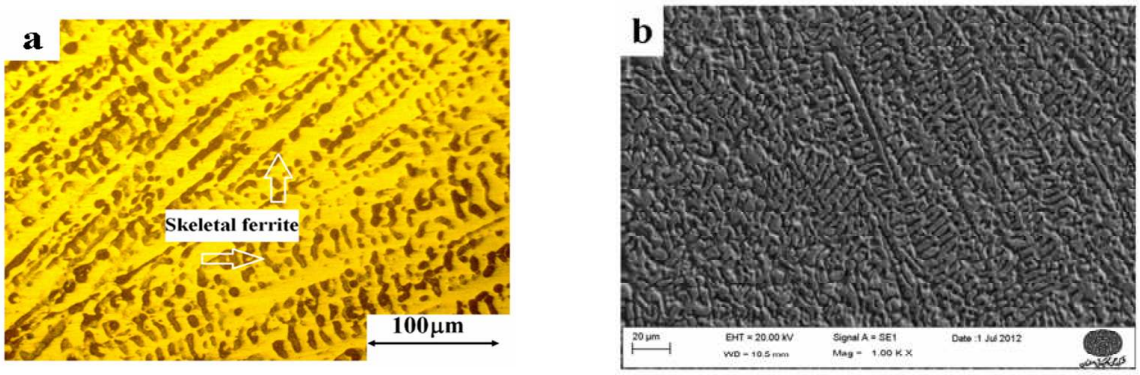

Fig. 3. Microstructure of weld metals ER309L, (a) optical microscopy (b) SEM.

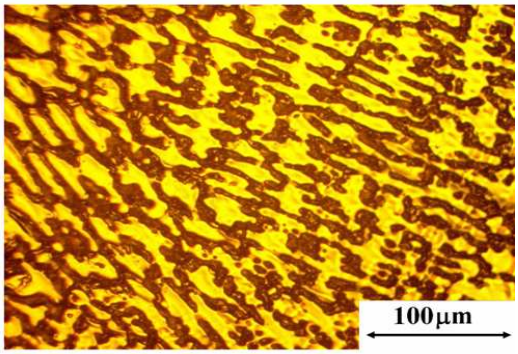

Fig. 4. Microstructure of weld metals ERNiCr-3.

chromium and nickel [17]. Based on Fig 7, in the Schaeffler diagram, A335 low alloy steel and 347 austenitic stainless steel base metals are shown by square sign, ER309L filler metal by circle sign and ERNiCr-3 by triangle sign. In 309L point toward the base metal, the weld metal is approximately in a place where the second contact line cuts the Iso-ferrite line which contains 5% ferrite. The studies showed that the control of weld metal ferrite content is important to predict cracking in several passes of the weld. ERNiCr-3 weld metal has a complete austenitic solidification because of the presence of nickel which is an austenitic promoter element. The austenite percent alterations of root pass for both used filler metals are shown in table 4 using a ferritescope. As it is observed, these results correspond to the results in Schaeffler diagram. The interface between 347 austenitic stainless steel and 309L weld metal is displayed in Fig 8. The morphology of delta ferrite which is solidified as a skeleton form is clearly observed in the image. Ferrite is formed in the grain boundaries [10]. When the Creq/ Nieq ratio is high, ferrite is more likely to be formed. There is a restriction in grain growth and also minimum susceptibility to HAZ liquation cracking possibility due to the ferrite produced in the HAZ grain boundaries [11]. The interface between A335 low alloy steel base metal and 309L weld metal is presented in Fig 9(a) and (b). The figure shows that the grain growth has occurred in the HAZ of low alloy steel which is planar. Moreover, in the transformation zone, melt boundary changes impressively in a very short distance (about 1 mm). There is a carbon migration from HAZ to the melt zone during the welding because of the change in the chemical composition of A335 which contains more carbon (Quintuple) than 309L weld metal [13]. The interface between 347 austenitic stainless steel base metal and ERNiCr-3 weld metal is shown in Fig 10(a) and (b). A continuous interface is observed all over the weld boundary which is of planar mode. An unmixed zone can be seen in a small fraction of the base metal because a part of the 347 austenitic stainless steel base metal, which is beside the melting pool, melts and then re-solidifies without dilution with the weld metal [14, 15]. Therefore, this zone has chemical composition of base metal, the unmixed zone is revealed in EDS result analysis, and the chemical composition of this zone is similar to 347 austenitic stainless steel [11, 16]. The interface between A335 low alloy steel base metal and ERNiCr-3 weld metal is displayed in Fig 11(a) and (b). In this figure, the grains growth in HAZ of A335 low alloy steel as well as the planar mode can be seen. The partially melting zone and the unmixed zone do not have

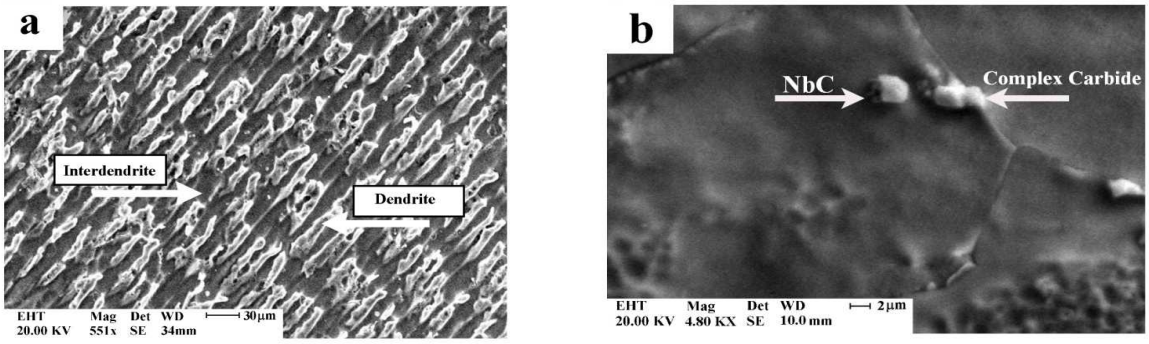

Fig. 5. SEM (a) Microstructure of weld metal ERNiCr-3, (b) Precipitition in weld metal of ERNiCr-3.

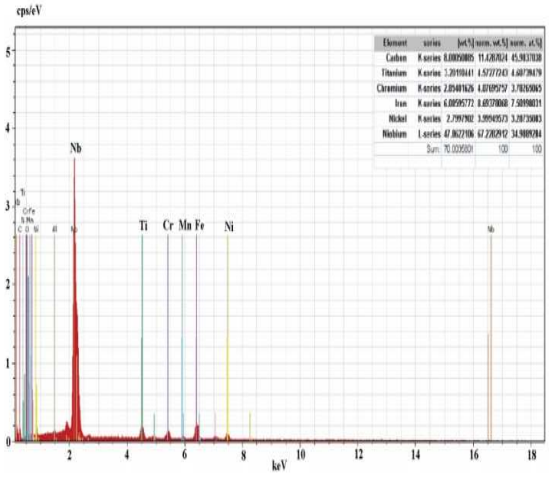

Fig. 6. EDS of deposits between dendritic of weld metal ERNiCr-3.

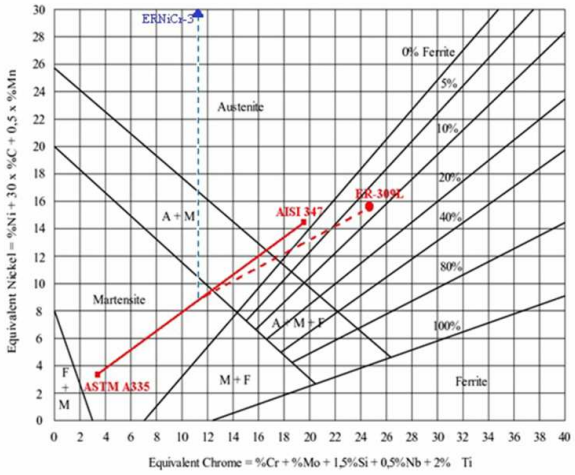

Fig. 7. Schaeffler Graph for both 309L and ERNiCr-3 filler metals.

Table 3. The calculated values of Cr_{eq}/ Ni_{eq} base and filler metals.

Creq/ Nieq values calculated			
Cr_{eq}/ Ni_{eq}	Ni_{eq}	Cr_{eq}	Type
1.39	14.05	19.52	AISI 347
0.99	3.15	3.12	ASTM A335
1.59	15.40	24.50	ER-309L
0.27	71.50	19.75	ER-NiCr-3

Table 4. Percentage changes of austenite for both weld filler metals.

Percent of error	Percentage of austenite	Filler metal
0.1	99.7	ERNiCr-3
1	94.5	ER309L

much width in this part of the joint [9]. As it was observed, we can gain a sound joint with suitable microstructure and properties for welding the two dissimilar steels discussed in this study with the two suggested filler metals and by following the above-mentioned welding parameters. Also, it was found that the weld metal ERNiCr-3 has a microstructure with primary austenite freezing and the weld metal 309L has a freezing in the form of primary ferrite. In addition, enlarging of the grains happened in HAZ of the two weld metals which contained bigger grains on the side of 347 stainless steel. In the interface of the ERNiCr-3 weld metal and both base metals, planer growth was observed in the interface of 309L weld metal and A335 base

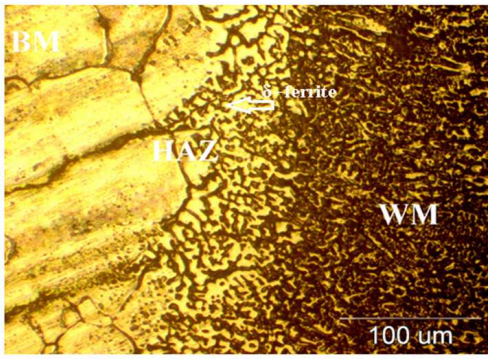

Fig. 8. Interface between the 309L weld metal and the 347 SS base metal.

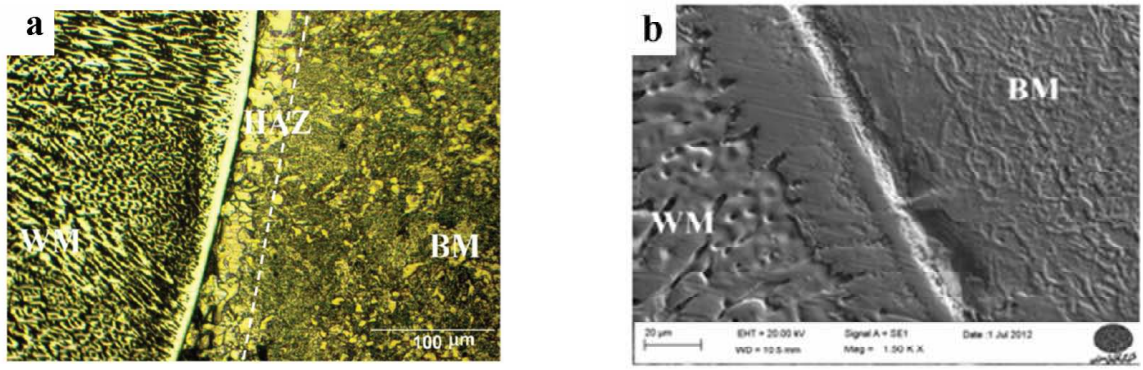

Fig. 9. Interfaces between the 309L weld metal and the A335 base metal (a) optical microscopy (b) SEM.

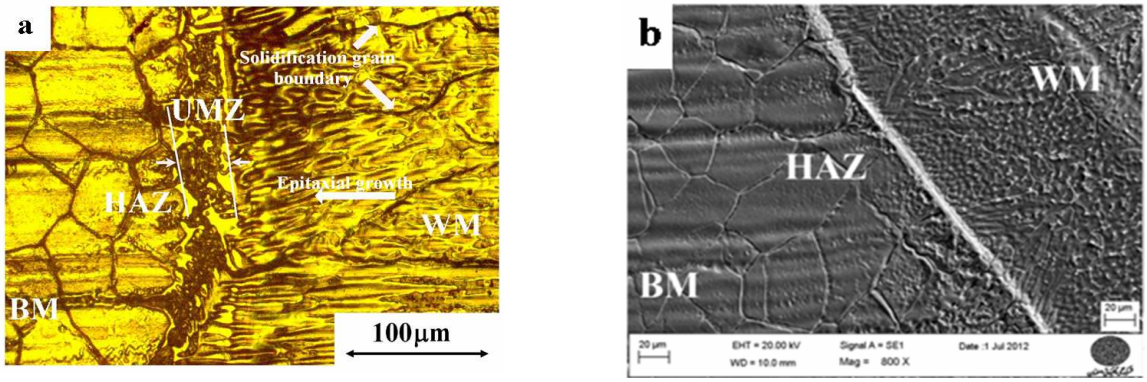

Fig. 10. Interfaces between the ERNiCr-3 weld metal and the 347 ss base metal (a) optical microscopy (b) SEM.

metal, planer growth was observed. With regard to similar studies, a study conducted by Omar, et al. can be mentioned. They welded carbon steel to austenite stainless steel with two weld metals 309 and Inconel 182 [18]. The results of their study showed that by using the nickel-based filler metal with pre-heat and controlling inter pass temperature we can remove the thin martensite layer which is produced in the interface of carbon steel and the weld metal because of austenite 309 stainless steel electrode. As it was mentioned before, in this study too, the thin martensite layer was seen in the low alloy steel side and after welding with 309L filler metal, and this layer was removed by using ER309 Weld metal. The proof of this claim was confirmed by conduction micro hardness measuring in Vickers [18]. On the other hand, because investigating the mechanical and corrosion properties of this dissimilar joint is of great importance in industry, in the rest of this study,

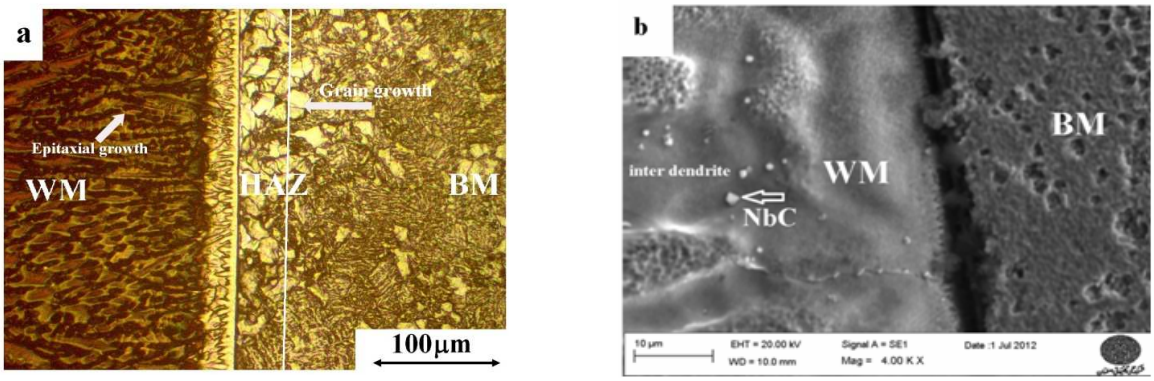

Fig. 11. Interfaces between the ERNiCr-3 weld metal and the A335 base metal (a) optical microscopy (b) SEM.

and in another article, the mechanical and corrosion properties of this dissimilar joint have been studied. The results of investigating the mechanical properties show tension strength and better resistance impact in low temperatures for ERNiCr-3 weld metal which supports the study conducted by ShahHosseini and Naffakh [1, 11]. Also, ERNiCr-3 weld metal has better resistance to pitting corrosion then; this improvement in resistance to pitting corrosion is due to alloy elements like a lot of Nickel, chrome and molybdenum [8, 12]. Finally, it can be denoted that for the joints between the AISI 347 austenitic stainless steel and A335low alloy steel, by the ERNICr-3 filler material provides the optimum qualities.

4. Conclusions

1. The solidification of ERNiCr-3 weld metal is similar to the primary austenite, and there is a two-phase structure which contains dendritic and interdendritic zones. The NbC precipitates and complex carbides are seen in the interdendritic zones. The microstructure of the ER309L weld metal includes primary ferrite with some austenite at the end of solidification which contains skeleton ferrite.
2. ERNiCr-3 weld metal has a complete austenitic solidification. The ferrite content of the root pass of 309L filler metal was about 5.7% by a ferritescope. These results correspond to the results in Schaeffler diagram.
3. There is a restriction in grain growth interface between 347 austenitic stainless steel and 309L weld metal and also minimum susceptibility to HAZ liquation cracking possibility due to the ferrite produced in the HAZ grain boundaries. An unmixed zone can be seen in interface between 347 austenitic stainless steel base metal and ERNiCr-3 weld metal.
4. There is a carbon migration from HAZ to the melt zone in the interface between A335 low alloy steel and 309L filler metal. The interface between A335 low alloy steel base metal and ERNiCr-3 weld metal is displayed partially melting zone and the unmixed zone do not have much width in this part of the joint.

References

1. H. ShahHosseini, M. Shamanian, A. Kermanpur, "Characterization of microstructures and mechanical properties of Inconel 617/310 stainless steel dissimilar welds", Mater Charact, vol. 62, 2011, pp.425-431.
2. ASM Handbook, Volume 1, "Properties and Selection: Irons, Steels, and High Performance Alloys", ASM International, Materials Park, Ohio, 2002.
3. J. C. Lippold, D. Koteki, "Welding Metallurgy and Weldability of Stainles Steels", John Wiley and Sons, New Jersey, 2005.
4. N. Arivazhagan, S. SurendraSingh, "Investigation on AISI 304 Austenitic Stainless Steel to AISI 4140 Low Alloy Steel Dissimilar Joints by Gas Tungsten Arc, Electron Beam and Friction Welding", Mater Des, vol. 32, 2011, pp. 3036–3050.
5. R. L. Klueh, L. King, "Austenitict Stainless Steel-Ferritic Steel Weld Joint Failures", Weld J, Vol. 61, 1982, pp. 302-311.
6. H. Muesch, "Welding of material grade TP 347", Nucl Eng Des, vol. 2, 2003, pp.

85:155-161.
7. G. Kaishu, X. Xiaodong, X. Hong, W. Zhiwen, "Effect of aging at 700 °c on precipitation and toughness of AISI 321 and AISI 347 austenitic stainless steel welds", Nucl Eng Des, vol. 23, 2005, pp. 2485–2494.
8. M. Tan, E. Akiyama, H. Habazaki, A. Kawashima, "The role of chromium and molybdenum in passivation of amorphous Fe-Cr-Mo-P-C alloys in deaerated 1 M HCl", Corros Sci, vol. 38, 1996, pp. 2137-2151.
9. V. Kumslyts, A. Vaclovas, "The Influence of Temperature-Time Parameter of Welded Joints Thermal Treatment on Strength-Related Characteristics Chromium-Molybdenum and Low Alloy Manganese Steels", Mat Science, vol. 13, 2007, pp. 123-126.
10. R. Dehmolaie, M. Shamanian, A. Kermanpour, "Microstructural characterization of dissimilar welds alloy 800 and HP heat – resistant steel", Mater Charact, vol. 59, 2008, pp. 1447-54.
11. H. Naffakh, M. Shamanian, F. Ashrafizadeh, "Dissimilar Welding of AISI 310 Austenitic Stainless Steel to Nickel-Based Alloy Inconel 657", J Mater Process Technol, vol. 209, 2008, 3628-3639.
12. M. Shimada, "intergranular corrosion resistant 304 stainless steel by twin-induced grain boundary engineering", Acta Mater, vol. 50, 2003, pp.2331-2341.
13. ASME Sec II, "Specification for Welding Rods, Electrodes and Filler Metals, Part C", American Society of Mechanical Engineers, 3rd ed., 2004.
14. L. LI, R. MESSLER, "Segregation of Phosphorus and Sulfur in Heat-Affected Zone Hot Cracking of Type 308 Stainless Steel", Weld J, 2002, pp. 78-84.
15. I. Haroe, A. Rosen, I. Hall, "Evolution of microstructure of AISI 347 stainless steel during heat treatment", MSTec, vol. 9, 1993, pp. 620-626.
16. A. L. Schaeffler, "Selection of Austenitic Electrodes for Welding Dissimilar Metals", Weld J, 1947, pp. 601-620.
17. ASME Sec IX, "Qualification Standard for Welding and Brazing Procedure", Article II, Welding Procedure Qualification, American Society of Mechanical Engineers, 2nd ed., 2001.
18. A. A. Omar, "Effects of Welding Parameters on Hard Zone Formation at Dissimilar Metal Welds", Weld J, Vol. 77, 1998, pp. 86-93.